Proc. VI Serbian-Bulgarian Astronomical Conference, Belgrade 7-11 May 2008,
Eds. M. S. Dimitrijević, M. Tsvetkov, L. Č. Popović, V. Golev
Publ. Astr. Soc. "Rudjer Bošković", No. 9, 2009, 335-342

RELATION BETWEEN NUCLEAR ACTIVITY, STAR FORMATION, AND BULGE MASS IN ACTIVE GALAXIES. I. EMISSION LINE PROPERTIES OF SEYFERT GALAXIES IN RBSC-NVSS SAMPLE

BOYKO MIHOV[1], LUBA SLAVCHEVA-MIHOVA[1], GEORGI PETROV[1]
and MICHEL DENNEFELD[2]

[1]*Institute of Astronomy, Bulgarian Academy of Sciences,*
72 Tsarigradsko Shose Blvd., 1784 Sofia, Bulgaria
e-mail: bmihov,lslav,petrov@astro.bas.bg
[2]*Institut d'Astrophysique de Paris, CNRS, and Université P. et M. Curie, 98bis Boulevard Arago, 75014 Paris, France*
e-mail: dennefel@iap.fr

Abstract. We propose to use a sub-sample extracted from the complete X-ray/radio RBSC-NVSS sample of AGNs to study the relationship between the properties of the optical emission lines and of the radio-to-X-ray continuum. Some preliminary results are presented.

1. INTRODUCTION

Boroson and Green (1992) introduced the eigenvector formalism in their landmark study of the optical emission line properties; see e.g. Sulentic et al. (2000, 2007, 2008) for a brief introduction to eigenvector formalism. Boroson and Green's (1992) Eigenvector 1 (E1) is dominated by the anti-correlation between FeII and [OIII] strengths. The leading interpretation is that E1 is driven by the Eddington ratio. The correlations between the properties of the optical emission lines and of the X-ray continuum were extensively studied: Vaughan et al. (2001) used a complete sample of Seyfert galaxies selected at 0.25 keV; Xu et al. (2003) used an X-ray sample defined by a high X-ray-to-optical ratio; Grupe (2004) used soft X-ray selected AGNs (see also Grupe et al. 1999).

It is important to note that each AGN sample has its own E1! AGN samples are constructed on the basis of certain observed properties, so, the correlations will be searched among different sets of observed parameters. This could put different weight to the different physical processes that drive the eigenvectors. For example, Boroson and Green's (1992) E1 is driven by the Eddington ratio, whereas Shang's

et al. (2003) E1 is driven by the Baldwin effect (see also Bachev et al. 2004). Therefore, the usage of different samples could improve the statistical significance of the correlations found and could help to improve our understanding of the physical processes driving the eigenvectors. New correlations could be searched for as well. For example, Wang et al. (2006) first extended the E1 relationships into infrared (IR) properties of AGNs: their E1 is dominated by the mid-IR colour $\alpha(60,25)$ and is related to the nuclear star formation history. According to them, the IR-dominated E1 can be interpreted as the ''age'' of an AGN.

We propose to use the complete X-ray/radio ROSAT Bright Source Catalog and the NRAO VLA Sky Survey (RBSC-NVSS) sample of AGNs in order to study the properties of the optical emission lines and of the radio-to-X-ray continuum; an IR Astronomical Satellite (IRAS) detected sub-sample of sources will be extracted. Working on our RBSC-NVSS sub-sample, we shall have the opportunity to study the correlations of the optical emission line properties with the radio and IR continuum properties in addition to the optical emission line/X-ray continuum correlations; the latter being most frequently studied. This will contribute to the present day knowledge about emission line/continuum correlations and about the physical processes that drive these correlations.

2. THE SAMPLE

We shall use the RBSC-NVSS sample of AGNs (Bauer et al. 2000). The RBSC-NVSS sample is a complete X-ray/radio sample defined by the following criteria:

- RBSC count rate $\geq$0.1 counts/s in the 0.1-2.4 keV band;
- Radio flux $\geq$2.5 mJy at 1.4 GHz;
- $\delta > -40°$;
- $|b| > 15°$.

In this way a sample of 1512 extragalactic objects was obtained that is comprised almost entirely of AGNs, making this the largest complete sample of its kind. The sample includes both radio-loud and radio-quiet AGNs thanks to deep VLA observations.

We extracted a sub-sample from the RBSC-NVSS sample using the following criteria:

- Radio flux <500 mJy to exclude the strongest radio sources;
- Only objects included in the IRAS catalogues (Faint Source and/or Point Source Catalogues);
- Only Seyfert galaxies.

In this way we got a sub-sample of 87 objects with radio, far-IR, and X-ray data. We list the programme objects and some basic information about them in Table 1.

Table 1. Equatorial coordinates (J2000), most common names, *B* magnitudes, redshifts, and Seyfert types of the programme objects.

#	α	δ	Name	*B*	z	Sy
1	00 02 25.94	+03 21 02.7	NGC 7811	15.1	0.0255	Sy1
2	00 06 19.45	+20 12 10.3	PG 0003+199	13.8	0.0256	Sy1
3	00 43 42.55	+37 25 19.6	IRAS F00409+3708	17.4	0.0799	Sy1
4	00 53 34.77	+12 41 33.8	UGC 00545	14.4	0.0611	Sy1
5	01 27 32.20	+19 10 45.1	UGC 01032	14.2	0.0174	Sy1.5
6	01 59 50.25	+00 23 38.9	PG 0157+001	15.7	0.1630	Sy1
7	02 00 26.37	+02 40 12.9	MRK 0584	15.3	0.0788	Sy1
8	02 28 14.40	+31 18 43.6	NGC 0931	14.5	0.0167	Sy1.5
9	02 32 33.14	+34 04 28.9	IRAS 02295+3351	16.3	0.0788	Sy1
10	02 38 27.77	+01 54 34.7	NGC 1019	14.3	0.0242	Sy1
11	03 53 46.90	+19 58 21.8	IC 0355	15.4	0.0292	Sy1
12	04 34 28.62	+71 28 05.2	IRAS 04288+7121	16.5	0.0248	Sy1.5
13	04 44 28.75	+12 21 11.4	IRAS 04416+1215	16.2	0.0889	Sy1
14	04 59 09.40	+04 58 29.7	UGC 03223	13.8	0.0156	Sy1
15	05 52 28.05	+59 28 32.1	IRAS 05480+5927	15.8	0.0585	Sy1
16	06 32 46.95	+63 40 25.6	UGC 03478	13.6	0.0128	Sy1
17	06 59 38.44	+54 11 45.0	MRK 0374	15.0	0.0435	Sy1
18	07 13 40.23	+38 20 38.1	IRAS F07102+3825	16.5	0.1227	Sy1
19	07 18 00.69	+44 05 27.4	IRAS F07144+4410	15.5	0.0614	Sy1
20	07 42 32.84	+49 48 34.1	UGC 03973	13.9	0.0222	Sy1
21	07 47 28.88	+60 56 00.4	UGC 04013	13.3	0.0293	Sy1
22	07 58 19.66	+42 19 43.5	IRAS F07548+4227	16.2	0.2100	Sy1
23	08 00 26.84	+10 13 15.6	IRAS 07577+1021	16.4	0.0478	Sy1.5
24	08 11 00.94	+76 02 45.6	PG 0804+761	15.1	0.1000	Sy1
25	08 15 16.68	+46 04 29.2	KUG 0811+462	15.2	0.0410	Sy1.5
26	08 38 10.93	+24 53 43.0	NGC 2622	15.0	0.0286	Sy1.8
27	08 54 39.25	+17 41 23.6	MRK 1220	16.5	0.0649	Sy1
28	09 13 45.43	+40 56 30.7	IRAS 09104+4109	18.0	0.4420	Sy2
29	09 18 26.05	+16 18 21.2	MRK 0704	15.4	0.0299	Sy1.5
30	09 37 03.65	+36 15 38.9	IRAS F09339+3629	17.7	0.1768	Sy1
31	09 45 54.49	+42 38 19.0	IRAS F09427+4252	16.3	0.0740	Sy2
32	09 47 05.02	+47 21 39.1	IRAS F09438+4735	18.1	0.5410	Sy1
33	10 05 41.03	+43 32 26.6	IRAS 10026+4347	16.5	0.1768	Sy1
34	10 17 18.72	+29 14 27.5	IRAS F10144+2929	15.8	0.0491	Sy1
35	10 34 38.57	+39 38 27.8	KUG 1031+398	15.6	0.0424	Sy1
36	10 40 43.77	+39 57 08.6	IRAS F10378+4012	16.0	0.1386	Sy2
37	10 44 39.13	+38 45 35.3	CGCG 212-045	14.9	0.0353	Sy1.5
38	10 50 35.90	+80 11 55.3	IRAS F10460+8027	16.1	0.1154	Sy1
39	10 58 01.15	+20 29 13.7	MRK 0634	15.9	0.0662	Sy1

40	11 13 49.71	+09 35 10.5	IC 2637	14.0	0.0292	Sy1.5
41	11 21 47.21	+11 44 18.4	PG 1119+120	15.1	0.0502	Sy1
42	11 24 08.74	+06 12 54.0	CGCG 039-167	14.9	0.0372	Sy1
43	11 36 29.17	+21 35 49.1	NGC 3758	15.2	0.0299	Sy1
44	11 41 15.87	+21 56 30.3	PG 1138+222	14.9	0.0632	Sy1
45	12 09 54.37	+06 28 10.5	IRAS F12073+0644	16.8	0.0796	Sy1.5
46	12 18 26.43	+29 48 47.3	NGC 4253	13.7	0.0129	Sy1.5
47	12 41 44.18	+35 03 49.0	NGC 4619	13.5	0.0231	Sy1
48	12 42 11.05	+33 17 12.3	IRAS F12397+3333	15.4	0.0435	Sy1.5
49	13 02 58.93	+16 24 27.4	MRK 0783	16.0	0.0672	Sy1.5
50	13 22 49.19	+54 55 30.4	RX J1322.8+5455	15.6	0.0640	Sy1
51	13 37 18.73	+24 23 02.8	[HB89] 1334+246	15.0	0.1076	Sy1
52	13 53 03.88	+69 18 28.7	UGC 08823	14.6	0.0294	Sy1.5
53	13 54 19.95	+32 55 47.7	UGC 08829	14.6	0.0260	Sy1
54	14 17 59.32	+25 08 13.5	NGC 5548	13.3	0.0172	Sy1.5
55	14 22 20.23	+29 42 55.0	IRAS 14201+2956	15.9	0.0530	Sy1
56	14 29 06.93	+01 17 06.3	PG 1426+015	17.5	0.0865	Sy1
57	14 31 05.05	+28 17 21.4	PG 1428+285	15.2	0.0458	Sy1
58	14 36 22.07	+58 47 41.6	UGC 09412	14.5	0.0315	Sy1.5
59	14 40 13.25	+61 56 43.4	IRAS F14390+6209	16.4	0.2760	Sy1
60	14 42 07.39	+35 26 24.9	PG 1440+356	14.9	0.0791	Sy1
61	14 47 33.01	+34 55 07.0	IRAS F14455+3507	17.1	0.6610	Sy1
62	15 07 44.43	+51 27 02.7	MRK 0845	15.6	0.0461	Sy1
63	15 14 20.53	+42 44 45.3	IRAS F15125+4255	16.0	0.1520	Sy
64	15 29 07.53	+56 16 09.1	IRAS F15279+5626	15.8	0.0990	Sy1
65	15 31 17.94	+07 27 29.1	NGC 5940	14.3	0.0337	Sy1
66	15 35 52.56	+57 54 16.7	PG 1534+580	15.2	0.0296	Sy1
67	15 58 18.21	+25 51 23.7	MRK 0864	16.5	0.0719	Sy2
68	15 59 10.07	+35 01 45.6	UGC 10120	14.6	0.0319	Sy1
69	16 11 24.57	+58 51 03.8	SBS 1610+589	15.8	0.0321	Sy1.5
70	16 13 01.69	+37 17 18.4	KUG 1611+374B	15.5	0.0696	Sy1
71	16 13 56.88	+65 43 10.4	PG 1613+658	15.2	0.1290	Sy1
72	16 14 13.20	+26 04 16.1	PG 1612+261	15.4	0.1310	Sy1.5
73	16 24 09.17	+26 04 34.3	IRAS F16221+2611	16.8	0.0400	Sy1
74	16 33 23.64	+47 18 59.9	IRAS 16319+4725	16.5	0.1163	Sy2
75	17 03 30.34	+45 40 47.5	IRAS 17020+4544	15.1	0.0604	Sy2
76	17 16 02.63	+31 12 08.6	IRAS F17141+3115	16.0	0.1110	Sy1
77	17 23 23.89	+36 30 13.3	IRAS 17216+3633	16.0	0.0400	Sy1
78	17 41 28.20	+03 48 52.4	IRAS F17389+0350	15.3	0.0300	Sy1
79	17 51 16.60	+50 45 36.4	IRAS 17500+5046	15.4	0.2997	Sy1
80	18 21 57.22	+64 20 36.4	[HB89] 1821+643	14.1	0.2970	Sy1
81	21 02 21.43	+10 58 18.3	CGCG 425-034	15.4	0.0287	Sy1.5
82	21 14 00.33	+82 04 52.0	IRAS F21166+8152	15.7	0.0840	Sy1

83	22 40 17.03	+08 03 15.1	UGC 12138	14.2	0.0246	Sy1.8
84	22 42 39.40	+29 43 33.6	UGC 12163	14.6	0.0240	Sy1
85	22 52 09.36	+26 42 39.7	IRAS 22497+2626	18.2	0.0670	Sy1
86	23 04 02.61	+22 37 25.5	MRK 0315	14.8	0.0389	Sy1.5
87	23 18 56.68	+00 14 37.2	NGC 7603	14.0	0.0295	Sy1.5

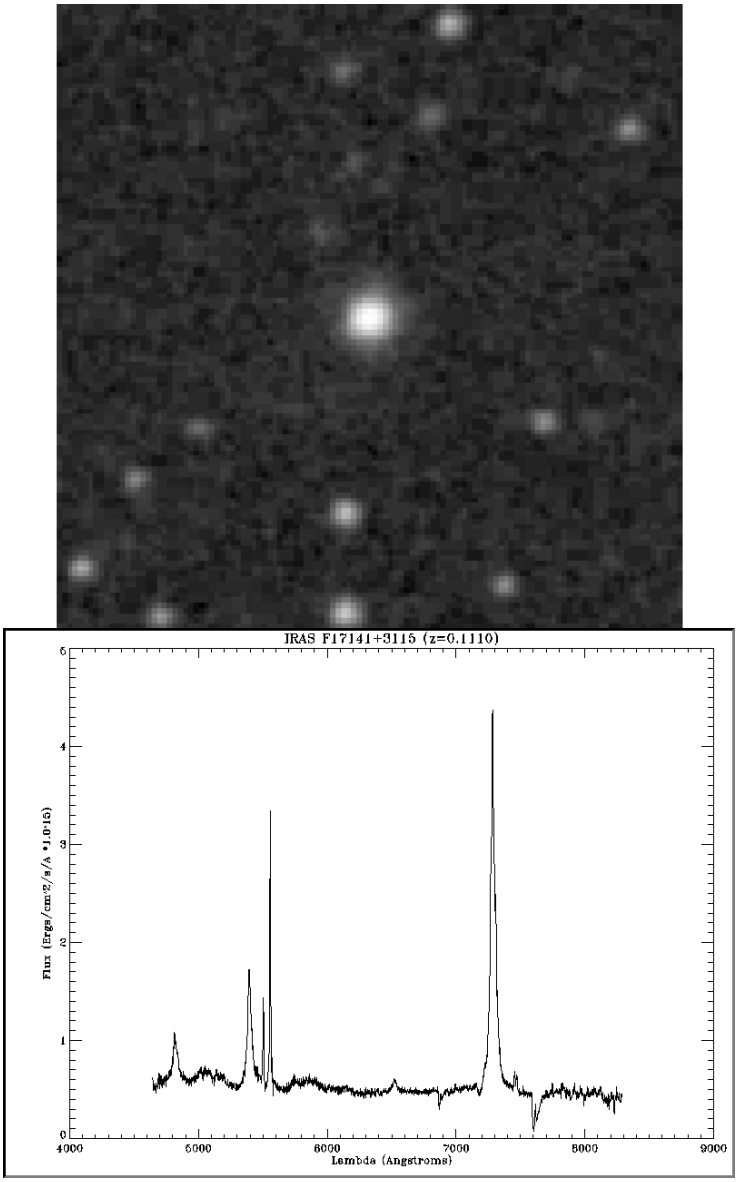

Figure 1: Upper panel: a 2×2 arcmin wide POSS-II red image of IRAS F17141+3115; North is at the top, East is to the left. Lower panel: a spectrum of the object taken at OHP.

2. PRELIMINARY RESULTS

We present preliminary results for two of the objects included in our sub-sample, namely IRAS F17141+3115 and IRAS F17389+0350. They were observed with the CARELEC spectrograph attached at the 1.93-m telescope of the Observatoire de Haute-Provence (OHP). Object images extracted from the digitized POSS-II and processed OHP spectra are presented in Figs. 1 and 2.

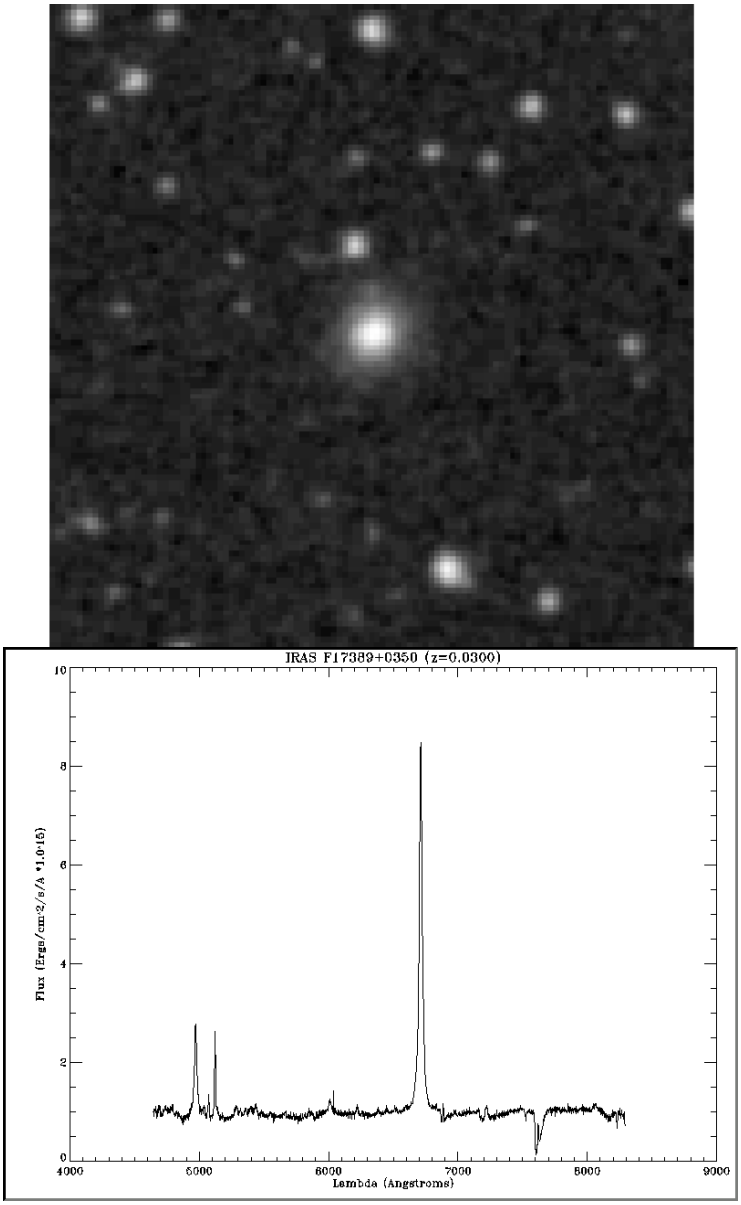

Figure 2: The same as in Fig. 1, but for IRAS F17389+0350.

We have also done a decomposition of the Hβ+[OIII] spectral region using unweighted 3-component Gaussian fit after subtraction of the FeII blends. The results are presented in Fig. 3. This decomposition should be considered as a trial one: the inclusion of more Gaussian components or the use of Lorentzian fitting function could be needed.

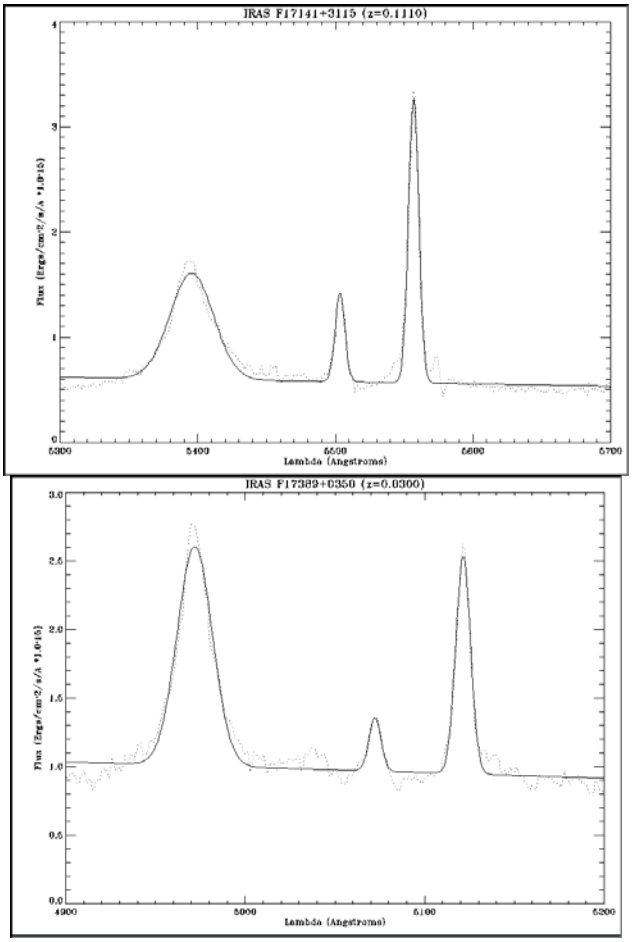

Figure 3: A decomposition of the Hβ+[OIII] spectral region (dots) using unweighted 3-component Gaussian fit (solid line) for IRAS F17141+3115 (upper panel) and for IRAS F17389+0350 (lower panel).

Acknowledgements

The Second Palomar Observatory Sky Survey (POSS-II) was made by the California Institute of Technology with funds from the National Science Foundation, the National Geographic Society, the Sloan Foundation, the Samuel Oschin Foundation, and the Eastman Kodak Corporation.

References

Bachev, R., Marziani, P., Sulentic, J. W., Zamanov, R., Calvani, M., Dultzin-Hacyan, D.: 2004, *Astrophys. J.*, **617**, 171.
Bauer, F. E., Condon, J. J., Thuan, T. X., Broderick, J. J.: 2000, *ApJS*, **129**, 547.
Boroson, T. A., Green, R. F.: 1992, *ApJS*, **80**, 109.
Grupe, D.: 2004, *Astron. J.,* **127**, 1799.
Grupe, D., Beuermann, K., Mannheim, K., Thomas, H.-C.: 1999, *Astron. Astrophys.*, **350**, 805.
Shang, Z., Wills, B. J., Robinson, E. L.. Wills, D., Laor, A., Xie, B., Yuan, J.: 2003, *Astrophys. J.*, **586**, 52.
Sulentic, J. W., Dultzin-Hacyan, D., Marziani, P.: 2007, *RMxAC*, **28**, 83.
Sulentic, J. W., Zamfir, S., Marziani, P., Dultzin, D.: 2008, *RMxAC*, **32**, 51.
Sulentic, J. W., Zwitter, T., Marziani, P., Dultzin-Hacyan, D.: 2000, *Astrophys. J.*, **536**, L5.
Vaughan, S., Edelson, R., Warwick, R. S., Malkan, M. A., Goad, M. R.: 2001, *Mon. Not. R. Astron. Soc.*, **327**, 673.
Wang, J., Wei, J. Y., He, X. T.: 2006, *Astrophys. J.*, **638**, 106.
Xu, D. W., Komossa, S., Wei, J. Y., Qian, Y., Zheng, X. Z.: 2003, *Astrophys. J.*, **590**, 73.